Biochemical and Biophysical Research Communications 399 (2010) 560–564

Contents lists available at ScienceDirect

Biochemical and Biophysical Research Communications

journal homepage: www.elsevier.com/locate/ybbrc

Tyrosine phosphorylation of vinculin at position 1065 modifies focal adhesion dynamics and cell tractions

Kevin Küpper [a], Nadine Lang [b], Christoph Möhl [a], Norbert Kirchgeßner [a], Simone Born [a], Wolfgang H. Goldmann [b,*], Rudolf Merkel [a], Bernd Hoffmann [a]

[a] Forschungszentrum Jülich GmbH, Institute of Bio- and Nanosystems 4, Jülich, Germany
[b] Center for Medical Physics and Technology, Biophysics Group, Friedrich-Alexander-University Erlangen-Nuremburg, Erlangen, Germany

ARTICLE INFO

Article history:
Received 26 July 2010
Available online 1 August 2010

Keywords:
Vinculin
Focal adhesion dynamics
Fluorescence recovery after photobleaching
Cell tractions
Tyrosine phosphorylation

ABSTRACT

Focal adhesions (FAs) connect the cellular actin cytoskeleton *via* integrin with the extracellular matrix. They comprise of many structural and signaling proteins which are highly dynamic, well regulated, and responsible for the sensing of physical properties from the environment. Vinculin is a protein that incorporates all these functions. Here, we investigated the phosphorylation of Y1065 in the activation/regulation of vinculin. We used different vinculin mutants mimicking either a permanently activated or inhibited phosphorylation site at position 1065. Using these mutants, we determined their influence on the exchange dynamics and cell forces using fluorescence recovery after photobleaching and traction microscopy. The results indicate that phosphorylation at Y1065 significantly increases the amount of freely exchanging vinculin within FAs whereas inhibition of this phosphorylation site leads to an uncontrolled exchange of vinculin and reduced adhesive cell forces. In conclusion, we show that phosphorylation on position Y1065 is essential for accurate incorporation of vinculin into FAs and mechanical behavior of cells.

1. Introduction

Cell contacts to the extracellular matrix (ECM) are vital for cell adhesion, spreading, migration, and survival. Most of these contacts are provided by the heterodimeric transmembrane integrin receptors that link the ECM to the cytoskeleton *via* focal adhesions (FAs) [1]. FAs are composed of a variety of different adaptor proteins, and their interaction defines the function of FAs [2,3]. Vinculin is one important adaptor protein that has been shown to associate with a number of proteins to transiently form FAs [4–6]. Furthermore, vinculin connects actin filaments *via* paxillin/talin to integrin and plays a central role in force transduction and mechanical stabilization of FAs [7–9]. However, its temporal activation and regulatory function still remains an open question.

Previous studies demonstrated that the formation and function of FAs largely depends on their protein composition [3,10]. It was reported that posttranslational changes like phosphorylation can modify the protein activity [5,11–13]. Cytoplasmic vinculin is in an autoinhibited, i.e. closed conformation, which is activated when binding to FAs [5,14]. Chen et al. demonstrated that vinculin undergoes a conformational change when incorporated into young FAs [15]. In addition, c-*src*-kinase phosphorylation of vinculin stabilizes the molecule's open conformation [12]. These authors identified tyrosine at position 100 and 1065 of vinculin as targets for the c-*src*-kinase. The phosphorylation by c-*src* may keep vinculin in a semi-stable conformation and enables it to bind to other proteins including Arp2/3, an actin nucleator and crosslinker [5,16]. These interactions reinforce the connection of the focal adhesion complex with the actin cytoskeleton, which allows cells to generate the appropriate prestress and strain energy for adequate cell adhesion and migration. We previously analyzed the influence of vinculin during cell migration and showed that the migratory capability of mouse embryonic fibroblasts (MEFs) mainly depends on adhesion strength -and dynamics as well as on the dynamics of cytoskeletal remodeling [17].

In our present study, we investigated the influence of vinculin phosphorylation at position tyrosine 1065 (Y1065) on the exchange dynamics in matured focal adhesions. We used mutant vinculin constructs, which either mimic a non-phosphorylated or permanently phosphorylated form at this position. To determine the differences in exchange dynamics of these vinculin mutants in focal adhesions compared to wildtype (WT) eGFP-vinculin, the constructs were expressed in MEF cells and analyzed by fluorescence recovery after photobleaching (FRAP). Employing traction microscopy, we also examined the contractile (adhesive) forces

* Corresponding author. Address: Friedrich-Alexander-University of Erlangen-Nuremberg, Center for Medical Physics and Technology, Biophysics Group, Henkestrasse 91, 91052 Erlangen, Germany. Fax: +49 (0) 9131 85 25601.
E-mail address: wgoldmann@biomed.uni-erlangen.de (W.H. Goldmann).

0006-291X/$ - see front matter © 2010 Elsevier Inc. All rights reserved.
doi:10.1016/j.bbrc.2010.07.110

of these cells. The results indicate that the phosphorylation of vinculin at position 1065 is not necessary for the recruitment to FAs, but essential for the timely activation of FAs and for the regulation of FA dynamics and cellular tractions.

2. Materials and methods

2.1. Cell lines and cell culture

Wildtype and vinculin-deficient ($vin^{-/-}$) mouse embryonic fibroblasts (MEFs) were a kind gift from Dr. E.D. Adamson (Burnham Institute, La Jolla, CA). The cell lines were cultured in high-glucose (4.5 g/l) Dulbecco's modified Eagle's medium with 4 mM L-glutamine supplemented with 10% fetal bovine serum and 100 U/ml penicillin/streptomycin (Sigma–Aldrich, Taufkirchen/Germany) and kept at 37 °C and 5% CO_2. For FRAP experiments, 2×10^5 cells were seeded in 35 mm diameter glass bottom culture dishes coated with 2.55 μg/cm^2 fibronectin (BD Bioscience, Erembodegem/Belgium).

2.2. Cloning and expression of vinculin constructs

Mouse wildtype vinculin (NCBI: BC008520) fused with enhanced green fluorescent protein (eGFP) was used as control and template for the exchange of mutant constructs. For this reason, the phosphorylatible amino acid tyrosine (Y) at position 1065 was replaced by phenylalanine (F) or glutamate (E), respectively, using site-directed mutagenesis. The exchange of tyrosine by phenylalanine (Y1065F) led to a vinculin mutant which cannot be phosphorylated at this position. In contrast, glutamate has similar charges than phosphorylated tyrosine and therefore mimics as Y1065E a permanently phosphorylated vinculin. Transfection was performed with 2 μg plasmid-DNA using Lipofectamine 2000 (Invitrogen, Karlsruhe/Germany) 24 h after seeding the cells. Cells were further incubated for 24–72 h before the experiment.

2.3. Localization control and immunostaining

Transfected cells were fixed for 20 min in 3.7% paraformaldehyde (Merck, Darmstadt/Germany) and afterwards permeabilized for 5 min at RT with 0.2% Triton X-100 in cytoskeleton-buffer (CB: 150 mM NaCl, 5 mM $MgCl_2$, 5 mM EGTA, 5 mM glucose, and 10 mM 2-(*N*-morpholino)ethanesulfonic acid at pH 6.1). After washing with CB, the cells were treated with blocking-solution (5% skimmed milk in CB) for 1 h at RT. Subsequently, cells were incubated for 45 min at 37 °C with a 1:100 solution of primary monoclonal mouse antibody against paxillin (Invitrogen, Karlsruhe/Germany). Cells were then washed three times with the blocking-solution. A secondary Cy3-labeled antibody against mouse (Jackson Immuno Research Europe Ltd., Suffolk/UK) was added (dilution 1:200 in blocking-solution). After additional incubation for 60 min at 37 °C, the cells were washed with CB and distilled water. Finally, they were embedded in 12 μl Gel-Mount/DABCO solution (Sigma–Aldrich, Taufkirchen/Germany). 10–20 randomly selected fields of view were recorded using a confocal microscope (LSM 510 meta) equipped with a Plan-Neofluar 40× NA 1.3 oil immersion objective (Carl Zeiss, Jena/Germany). eGFP was excited at 488 nm, and the emitted light was detected between 505 and 530 nm. Light from Cy3 was detected between 560 and 615 nm after 543 nm excitation using a helium–neon laser. The intensity profiles of single focal adhesions were determined by the profile tool in ImageJ (National Institute of Health) and plotted in Matlab (The Mathworks, Natick, MA). The line profiles were averaged over a line width of 10 pixels which equals 1.5 μm.

2.4. Fluorescence recovery after photobleaching (FRAP)

Binding kinetics of eGFP–vinculin proteins within FAs of living cells were determined by FRAP. In brief, an intense pulse of illumination light at the excitation wavelength of the fluorophore was applied to a single FA. This bleached a major fraction of the fluorophore within the illuminated area, mostly without altering the protein structure and function. The kinetic exchange rate of vinculin was determined by measuring the replacement of photo-bleached *vs.* fluorescent molecules over time. Prior to FRAP measurements, cells were observed for at least 5 min and only stable FAs present over the entire period were analyzed. Since the detected fluorescence recovery of FAs is an overlay of both, protein binding kinetics within and free diffusion above FAs [13], we used total internal reflection fluorescence (TIRF) laser illumination on an Axio Observer Z.1 (Carl Zeiss, Jena/Germany) to reduce the influence of freely diffusing, cytoplasmic vinculin. The microscope was equipped with an XL-incubation chamber for live cell imaging. For spot bleaching, an additional diode laser (473 nm, 100 mW; Rapp OptoElectronic, Hamburg/Germany) was coupled into the microscope *via* a multimode optical fiber (550 μm diameter), resulting in a bleach spot of 5 μm. Images were taken for 60 s before and 300 s after bleaching of a single FA (acquisition rate: 15 images/min), using an alpha-Plan-Apochromat 100× NA 1.46 objective (Carl Zeiss, Jena/Germany). Note that bleaching was carried out with 60% laser power output for 1.5 s.

As previously mentioned, lateral diffusion of cytosolic molecules and dissociation/association processes of spatially fixed binding sites in FAs occur simultaneously. Under these conditions, the diffusion related fluorescence recovery is much faster than the fluorescence recovery due to binding kinetics [13]. To exclude diffusion related recovery from the fluorescence signal, I_{Ad} the signal was corrected for the contribution of cytosolic molecules. Moreover, the time series were corrected for continuous, unintentional bleaching of the complete image due to the observation light. The cytosolic background, I_{Cyt} was calculated at each time point from the average intensity of the cell outside focal adhesions. Continuous bleaching was monitored by determining the average fluorescence intensity, I_{Ref} of several non-bleached adhesions. The corrected recovery curve, I_C was calculated according to

$$I_C = \frac{I_{Ad} - I_{Cyt}}{I_{Ref} - I_{Cyt}}. \quad (1)$$

The corrected recovery curves were normalized for comparison of individual measurements. To this end, the average value of I_C before bleaching, I_0 was determined as well as the intensity immediately after bleaching, I_{BI}. The normalized recovery curve $n(t)$ was calculated according to

$$n(t) = \frac{I_C - I_{BI}}{I_0 - I_{BI}}. \quad (2)$$

Since the normalized recovery was due to binding/unbinding reactions, the measured normalized recovery curve $n(t)$ was fitted to a first order exponential, describing a single exchange kinetics model

$$n(t) = \alpha(1 - e^{-\kappa t}) \quad (3)$$

where, κ is the rate of recovery and, α is the fraction of exchanging molecules [13]. All intensities were extracted from raw image data, using ImageJ (National Institute of Health). FRAP calculations were carried out in MatLab 2009 (The Mathsworks, Natick, MA).

2.5. Traction microscopy

Gels for traction experiments were cast on rectangular 75 × 25 mm non-electrostatic silane-coated glass slides [18]. Gels

with 6.1% acrylamide/0.24% bis-acrylamide were used. The Young's modulus of the gels was around 13 kPa. Yellow-green fluorescently carboxylated beads with a diameter of 0.5 μm (Invitrogen, Karlsruhe/Germany) were suspended in the gels and centrifuged at 300*g* towards the gel surface during polymerization at 4 °C [8]. These beads served as marker for gel deformation. The surface of the gel was activated with Sulfo-SANPAH (Pierce Biotechnology, Bonn/Germany) and coated with 50 μg/ml Collagen I (Biochrom, Berlin/Germany). The cell suspension added to the gel was contained in a silicone ring (flexi-perm, In Vitro, Göttingen, Germany) attached to the glass slide. Cell tractions were computed from an unconstrained deconvolution of the gel surface displacement field measured before and after cell detachment with 8 μM cytochalasin D in a trypsin/EDTA solution [19]. Gel deformations were estimated using a Fourier-based difference-with-interpolation image analysis [20].

3. Results

We recently showed that the phosphorylation of vinculin at position tyrosine 1065 (Y1065) is a spatiotemporal process and correlates with young, developing FAs whereas matured, stable FAs show much less phosphorylation of vinculin [13]. These findings suggest that the transient phosphorylation of vinculin might play an important role during FA assembly, a process of highly regulated protein dynamics [3,21]. Furthermore, our earlier data showed that the exchange dynamics of vinculin in FAs of keratinocytes decreases with the state of FA maturation. To analyze these findings in more detail, we performed vinculin exchange dynamics measurements on different vinculin Y1065 constructs using FRAP. Beside vinculin in its wildtype form, we used a mutant where Y1065 was genetically replaced by glutamate (Y1065E) to mimic permanently phosphorylated vinculin or replaced by phenylalanine (Y1065F) to mimic phosphorylation inhibited vinculin. Control experiments showed that all three vinculin constructs were localized in FAs after expression in MEF vin$^{-/-}$ cells (Fig. 1), which indicated that neither phosphorylation of Y1065 nor its regulation was crucial for vinculin recruitment. However, the ratio between freely diffusing and incorporated vinculin seemed to be lower for the inhibited mutant (Y1065F) (data not shown).

Since MEFs are less motile than keratinocytes, they lack a pronounced polarity and generally exhibit more stable, fully matured than younger FAs. Therefore, we performed FRAP measurements only on stable, matured FAs at an age of at least 5 min. Using Eq. (3), we determined α as the amount of exchanging vinculin in FAs. This so-called mobile fraction of vinculin was compared between the different vinculin mutants. As control, we first investigated the incorporation of WT vinculin. The FRAP curve (averaged from 17 independent measurements) showed a mobile fraction of 63% for wildtype vinculin (Fig. 2). The exchange was compared to that of permanently phosphorylated vinculin (Y1065). Since we identified vinculin Y1065 phosphorylation mainly in nascent, highly dynamic FAs of keratinocytes [13], we expected an increase in the mobile fraction for the permanently phosphorylated Y1065E construct. Indeed, the averaged FRAP curve (out of 18 independent experiments) revealed a significantly higher mobile fraction of 76% for Y1065E compared to wildtype vinculin. Note that the distribution of single measurements are shown in the box plots α to Fig. 2.

To answer the question of whether the inhibition of Y1065 phosphorylation alters the dynamics of vinculin insertion in FAs in a reverse manner, we analyzed the exchange dynamics of phosphorylation inhibited (Y1065F) vinculin. As described before, our investigations were carried in matured FAs, exhibiting barely phosphorylated vinculin. We therefore assumed comparable exchange dynamics for WT vinculin and Y1065F mutants. As expected, we obtained similar mobile fractions for Y1065F (59%) and WT vinculin (63%) from the averaged recovery curves. However, the mobile fractions for the single measurements of the Y1065F mutant showed a much broader distribution compared to WT vinculin, which points to an uncontrolled exchange of vinculin Y1065F in focal adhesions (Fig. 2).

To gain further insight into the cellular effects of vinculin's Y1065F uncontrolled exchange, we performed additional traction microscopy measurements since vinculin is known to be involved in force regulation of FAs [8,22–24]. Hence, the uncontrolled exchange of vinculin might also influence the force generation in

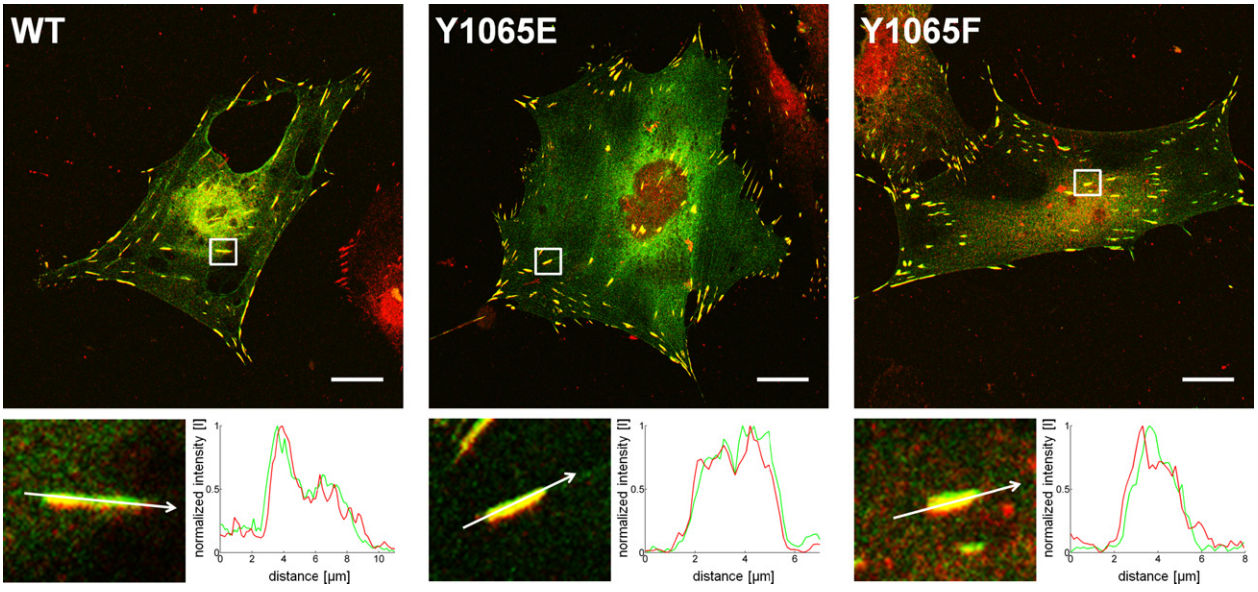

Fig. 1. Incorporation of vinculin mutants. eGFP labeled WT (left), Y1065E (middle), and Y1065F (right) vinculin were expressed in vin$^{-/-}$ MEF cells. Cells were fixed and subsequently analyzed for vinculin (green) and paxillin (red). Scale bar = 20 μm. The graphs at the lower right of each image represents the normalized intensity profile [I] of both proteins along with the indicated arrow for the enlarged focal adhesions (lower left) marked in the overview image. Note that the images were gamma-contrast enhanced for visualization. (For interpretation of the references to colour in this figure legend, the reader is referred to the web version of this article.)

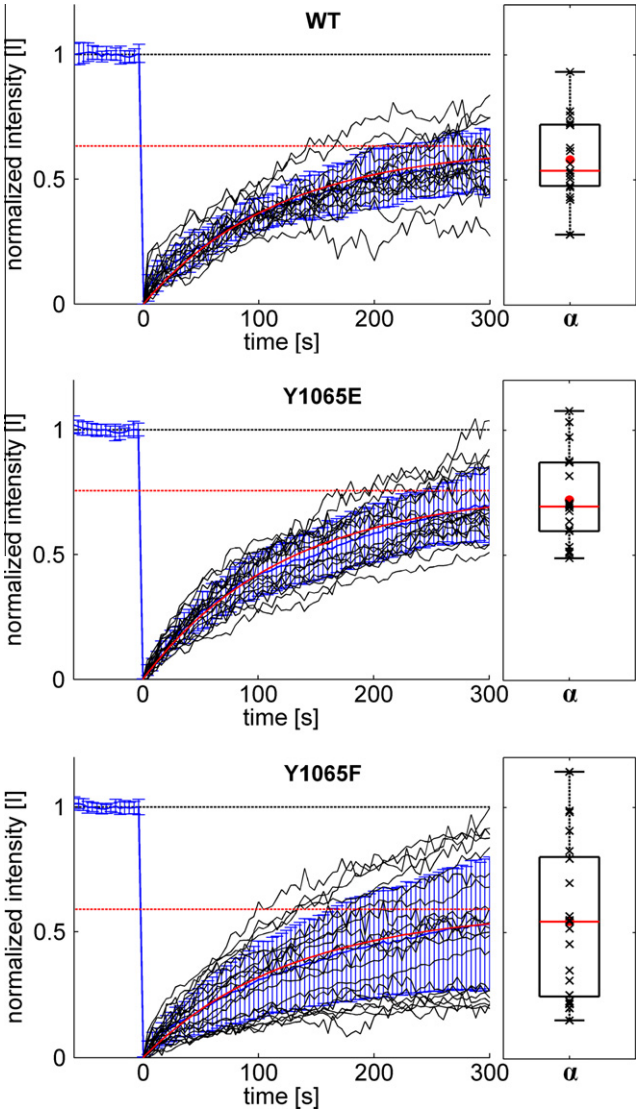

Fig. 2. Exchange dynamics of different vinculin constructs. eGFP-WT, Y1065E, and Y1065F vinculin constructs were expressed in vin$^{-/-}$ cells for FRAP measurements. Before bleaching, cells were monitored for at least 5 min to ensure that only mature FAs at a minimum age of 5 min were analyzed. Black graphs show the normalized intensity [I] curves from individual measurements. The mean value and the standard deviation σ are shown in blue; results from the curve fit (Eq. (3)) of mean values are shown in red. The saturation value, α indicates the mobile fraction (red dotted line). At the right of each graph, the box plots show the distribution of the mobile fractions of single measurements (black "x"), where the bottom and the top of each box indicates the 25th and 75th percentile. The mean values are given as a red dot, the median as a red line. Number of measured cells: WT vinculin ($n = 17$), Y1065E mutant ($n = 18$), and Y1065F mutant ($n = 23$). (For interpretation of the references to colour in this figure legend, the reader is referred to the web version of this article.)

cells. In fact, cells expressing the Y1065F mutant applied significantly lower forces to the substrate than cells expressing WT vinculin (Fig. 3). In conclusion, our results strongly argue for a crucial relevance of a timely regulated vinculin phosphorylation/dephosphorylation at tyrosine 1065 for the activation of vinculin to functionally regulate FA formation and cell force application.

4. Discussion

FAs are complex structures and their function is defined by the composition and interaction of the participating proteins. Consequently, the assembly of FAs is subject to a precise temporal

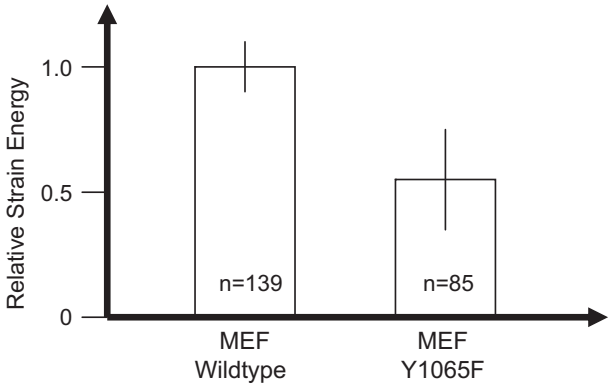

Fig. 3. Traction microscopy. The relative strain energy of wildtype vinculin and Y1065F mutant expressed in MEFs. Note that '*n*' indicates the number of cells measured, and that the error bars denote the mean ± SE. The value for MEF wildtype strain energy is around 0.8 pJ [8].

control. Defects in the regulation can lead to serious problems and affect cellular behavior. Zhang et al. [12] and Moese et al. [16] have both argued that tyrosine phosphorylation of vinculin plays an important role in the early development of FAs. It is believed that upon activation, vinculin remains first in a semi-stable state at which PIP_2 and other membrane phospholipids interact with its C-terminal tail [5,6,8,14,25–27].

Y1065 is located at the C-terminus end of vinculin, and its c-*src*-dependent phosphorylation is known to be transient [12,13]. Thus, pY1065 may have a regulatory function during the first activation steps of vinculin. In nascent FAs, vinculin shows a high exchange dynamics and higher mobile fractions compared to matured FAs, where the amount of phosphorylated Y1065 vinculin is lower. Furthermore, in matured FAs, vinculin shows more stable interactions with the actin cytoskeleton and reduced exchange dynamics [13,15]. This is indicative that phosphorylation at position Y1065 is connected with the activation of vinculin.

In the present study, we analyzed the influence of Y1065 phosphorylation on vinculin exchange dynamics in a more direct fashion by comparing the exchange dynamics of different vinculin mutants using the FRAP technique. Although vinculin recruitment to FAs does not seem to be altered by the mutation at position Y1065 (Fig. 1), our FRAP measurements strongly indicate a regulative influence of Y1065 phosphorylation (Fig. 2). As shown, the exchangeable, mobile fraction of vinculin in matured FAs is significantly increased in cells expressing Y1065E constructs. In contrast, inhibition of phosphorylation at this position leads to uncontrolled exchange dynamics of vinculin. The strong cellular effect by inhibition of just one single vinculin phosphorylation site was further confirmed by traction experiments (Fig. 3). Here, cells expressing the phosphorylation inhibited vinculin mutant (Y1065F) showed a significant decrease in strain energy compared to cells expressing WT vinculin. These findings imply that c-*src*-kinase phosphorylation of vinculin at position Y1065 is not essential for vinculin recruitment, but affects the FA formation by keeping vinculin in a highly exchangeable state. This could further increase the interaction with other binding partners, including membrane phospholipids and proteins like the actin crosslinker Arp2/3 [8,16]. After vinculin's association, it might become dephosphorylated, which in turn could lead to a strengthening of the binding and consequently to a reduced exchange dynamics of vinculin and increased traction forces *via* FAs. Therefore, a higher mobile fraction of vinculin is favorable only for young FAs, where high protein dynamics are essential for correct FA organization and assembly [13,28]. However, mature FAs exert strong forces, i.e. high protein dynamics is unwanted. At this point, we can only speculate about the

wide distribution in exchange dynamics for the non-phosphorylatible vinculin construct. It seems that this mutation leads to highly uncoordinated vinculin incorporation into FAs and interaction with other binding partners.

In summary, we have shown that phosphorylation of vinculin at position Y1065 is not essential for the formation of FAs, but that it has a strong influence on vinculin dynamics in FAs and ultimately on the function of FAs in force transmission. Therefore, vinculin can be regarded as an important regulator for FA maturation and coupler of the actin cytoskeleton to the extracellular matrix. Better understanding of the activation of vinculin and its regulatory function will give further insight into FA signaling and consequently to cell behavior.

Acknowledgments

We thank Dr. E.D. Adamson for providing the MEF cells and Dr. B. Fabry for stimulating discussions. We are also indebted to the entire team of IBN 4 for their interlectual input. This work was supported by grants from Bayerisch-Französisches Hochschulzentrum, Deutscher Akademischer Austausch Dienst, Bavaria California Technology Center, Deutsche Forschungsgemeinschaft (GO598/13-1), and Bundesministerium für Bildung und Forschung (Program 0315501).

References

[1] R.O. Hynes, Integrins: bidirectional, allosteric signaling machines, Cell 110 (2002) 673–687.
[2] D.R. Critchley, Focal adhesions – the cytoskeletal connection, Curr. Opin. Cell Biol. 12 (2000) 133–139.
[3] E. Zamir, B. Geiger, Molecular complexity and dynamics of cell–matrix adhesions, J. Cell Sci. 114 (2001) 3583–3590.
[4] W.H. Goldmann, Mechanical aspects of cell shape regulation and signaling, Cell Biol. Int. 26 (2002) 313–317.
[5] K.A. Demali, Vinculin – a dynamic regulator of cell adhesion, Trends Biochem. Sci. 29 (2004) 565–567.
[6] W.H. Ziegler, R.C. Liddington, D.R. Critchley, The structure and regulation of vinculin, Trends Cell Biol. 16 (2006) 453–460.
[7] C.T. Mierke, P. Kollmannsberger, D. Paranhos-Zitterbart, J. Smith, B. Fabry, W.H. Goldmann, Mechano-coupling and regulation of contractility by the vinculin tail domain, Biophys. J. 94 (2008) 661–670.
[8] G. Diez, P. Kollmannsberger, C.T. Mierke, T.M. Koch, H. Vali, B. Fabry, W.H. Goldmann, Anchorage of vinculin to lipid membranes influences cell mechanical properties, Biophys. J. 97 (2009) 3105–3112.
[9] C. Grashoff, B.D. Hoffman, M.D. Brenner, R. Zhou, M. Parsons, M.T. Yang, M.A. McLean, S.G. Sligar, C.S. Chen, T. Ha, M.A. Schwartz, Measuring mechanical tension across vinculin reveals regulation of focal adhesion dynamics, Nat. Lett. 466 (2010) 263–267.
[10] R. Zaidel-Bar, C. Ballestrem, Z. Kam, B. Geiger, Early molecular events in the assembly of matrix adhesions at the leading edge of migrating cells, J. Cell Sci. 116 (2003) 4605–4613.
[11] E. Zamir, B.Z. Katz, S. Aota, K.M. Yamada, B. Geiger, Z. Kam, Molecular diversity of cell–matrix adhesions, J. Cell Sci. 112 (Pt 11) (1999) 1655–1669.
[12] Z. Zhang, G. Izaguirre, S.Y. Lin, H.Y. Lee, E. Schaefer, B. Haimovich, The phosphorylation of vinculin on tyrosine residues 100 and 1065, mediated by SRC kinases, affects cell spreading, Mol. Biol. Cell 15 (2004) 4234–4247.
[13] C. Möhl, N. Kirchgessner, C. Schäfer, K. Küpper, S. Born, G. Diez, W.H. Goldmann, R. Merkel, B. Hoffmann, Becoming stable and strong: the interplay between vinculin exchange dynamics and adhesion strength during adhesion site maturation, Cell Motil. Cytoskeleton 66 (2009) 350–364.
[14] C. Bakolitsa, J.M. de Pereda, C.R. Bagshaw, D.R. Critchley, R.C. Liddington, Crystal structure of the vinculin tail suggests a pathway for activation, Cell 99 (1999) 603–613.
[15] H. Chen, D.M. Cohen, D.M. Choudhury, N. Kioka, S.W. Craig, Spatial distribution and functional significance of activated vinculin in living cells, J. Cell Biol. 169 (2005) 459–470.
[16] S. Moese, M. Selbach, V. Brinkmann, A. Karlas, B. Haimovich, S. Backert, T.F. Meyer, The *Helicobacter pylori* CagA protein disrupts matrix adhesion of gastric epithelial cells by dephosphorylation of vinculin, Cell Microbiol. 9 (2007) 1148–1161.
[17] C.T. Mierke, P. Kollmannsberger, D.P. Zitterbart, G. Diez, T.M. Koch, S. Marg, W.H. Ziegler, W.H. Goldmann, B. Fabry, Vinculin facilitates cell invasion into three-dimensional collagen matrices, J. Biol. Chem. 285 (2010) 13121–13130.
[18] R.J. Pelham Jr., Y.L. Wang, Cell locomotion and focal adhesions are regulated by the mechanical properties of the substrate, Biol. Bull. 194 (1998) 348–349. discussion 349–350.
[19] J.P. Butler, I.M. Tolic-Norrelykke, B. Fabry, J.J. Fredberg, Traction fields, moments, and strain energy that cells exert on their surroundings, Am. J. Physiol. Cell Physiol. 282 (2002) C595–C605.
[20] C. Raupach, D.P. Zitterbart, C.T. Mierke, C. Metzner, F.A. Muller, B. Fabry, Stress fluctuations and motion of cytoskeletal-bound markers, Phys. Rev. E Stat. Nonlin. Soft Matter Phys. 76 (2007) 011918.
[21] B. Geiger, A. Bershadsky, Assembly and mechanosensory function of focal contacts, Curr. Opin. Cell Biol. 13 (2001) 584–592.
[22] R.M. Ezzell, W.H. Goldmann, N. Wang, N. Parasharama, D.E. Ingber, Vinculin promotes cell spreading by mechanically coupling integrins to the cytoskeleton, Exp. Cell Res. 231 (1997) 14–26.
[23] J.D. Humphries, P. Wang, C. Streuli, B. Geiger, M.J. Humphries, C. Ballestrem, Vinculin controls focal adhesion formation by direct interactions with talin and actin, J. Cell Biol. 179 (2007) 1043–1057.
[24] C.T. Mierke, The role of vinculin in the regulation of the mechanical properties of cells, Cell Biochem. Biophys. 53 (2009) 115–126.
[25] J. Weekes, S.T. Barry, D.R. Critchley, Acidic phospholipids inhibit the intramolecular association between the N- and C-terminal regions of vinculin, exposing actin-binding and protein kinase C phosphorylation sites, Biochem. J. 314 (Pt 3) (1996) 827–832.
[26] V.F. Wirth, F. List, G. Diez, W.H. Goldmann, Vinculin's C-terminal region facilitates phospholipid membrane insertion, Biochem. Biophys. Res. Commun. 398 (2010) 433–437.
[27] W.H. Goldmann, Correlation between the interaction of the vinculin tail domain with lipid membranes, its phosphorylation and cell mechanical behaviour, Cell Biol. Int. 34 (2010) 339–342.
[28] B. Geiger, A. Bershadsky, R. Pankov, K.M. Yamada, Transmembrane crosstalk between the extracellular matrix–cytoskeleton crosstalk, Nat. Rev. Mol. Cell Biol. 2 (2001) 793–805.